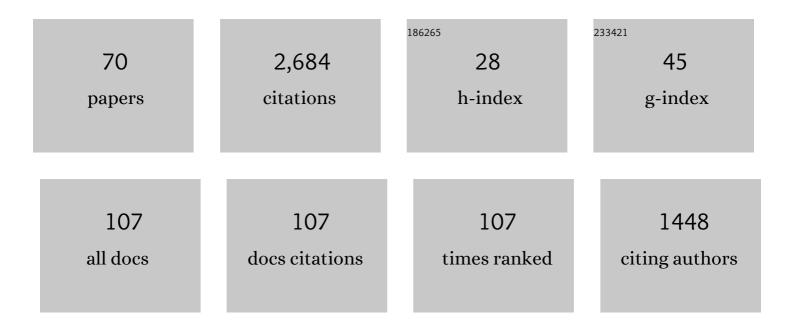
Reinhold Spang

List of Publications by Year in descending order

Source: https://exaly.com/author-pdf/3584774/publications.pdf Version: 2024-02-01



#	Article	IF	CITATIONS
1	A new Chemical Lagrangian Model of the Stratosphere (CLaMS) 1. Formulation of advection and mixing. Journal of Geophysical Research, 2002, 107, ACH 15-1.	3.3	228
2	MIPAS level 2 operational analysis. Atmospheric Chemistry and Physics, 2006, 6, 5605-5630.	4.9	174
3	Colour indices for the detection and differentiation of cloud types in infra-red limb emission spectra. Advances in Space Research, 2004, 33, 1041-1047.	2.6	132
4	Cryogenic Infrared Spectrometers and Telescopes for the Atmosphere (CRISTA) data processing and atmospheric temperature and trace gas retrieval. Journal of Geophysical Research, 1999, 104, 16349-16367.	3.3	130
5	Horizontal water vapor transport in the lower stratosphere from subtropics to high latitudes during boreal summer. Journal of Geophysical Research D: Atmospheres, 2013, 118, 8111-8127.	3.3	100
6	Ammonium nitrate particles formed in upper troposphere from ground ammonia sources during Asian monsoons. Nature Geoscience, 2019, 12, 608-612.	12.9	95
7	Reconciliation of essential process parameters for an enhanced predictability of Arctic stratospheric ozone loss and its climate interactions (RECONCILE): activities and results. Atmospheric Chemistry and Physics, 2013, 13, 9233-9268.	4.9	88
8	Gimballed Limb Observer for Radiance Imaging of the Atmosphere (GLORIA) scientific objectives. Atmospheric Measurement Techniques, 2014, 7, 1915-1928.	3.1	85
9	The CRISTA-2 mission. Journal of Geophysical Research, 2002, 107, CRI 1-1-CRI 1-12.	3.3	84
10	Spectroscopic evidence for NAT, STS, and ice in MIPAS infrared limb emission measurements of polar stratospheric clouds. Atmospheric Chemistry and Physics, 2006, 6, 1201-1219.	4.9	82
11	Envisat MIPAS measurements of CFC-11: retrieval, validation, and climatology. Atmospheric Chemistry and Physics, 2008, 8, 3671-3688.	4.9	77
12	GLObal limb Radiance Imager for the Atmosphere (GLORIA): Scientific objectives. Advances in Space Research, 2005, 36, 989-995.	2.6	68
13	Polar stratospheric cloud observations by MIPAS on ENVISAT: detection method, validation and analysis of the northern hemisphere winter 2002/2003. Atmospheric Chemistry and Physics, 2005, 5, 679-692.	4.9	66
14	Lagrangian simulations of the transport of young air masses to the top of the Asian monsoon anticyclone and into the tropical pipe. Atmospheric Chemistry and Physics, 2019, 19, 6007-6034.	4.9	57
15	Formation of solid particles in synoptic-scale Arctic PSCs in early winter 2002/2003. Atmospheric Chemistry and Physics, 2004, 4, 2001-2013.	4.9	54
16	CRISTA observations of cirrus clouds around the tropopause. Journal of Geophysical Research, 2002, 107, CRI 2-1-CRI 2-18.	3.3	51
17	First results of MIPAS/ENVISAT with operational Level 2 code. Advances in Space Research, 2004, 33, 1012-1019.	2.6	51
18	Polar Stratospheric Clouds: Satellite Observations, Processes, and Role in Ozone Depletion. Reviews of Geophysics, 2021, 59, e2020RG000702.	23.0	49

REINHOLD SPANG

#	Article	IF	CITATIONS
19	Observations of a distinctive infra-red spectral feature in the atmospheric spectra of polar stratospheric clouds measured by the CRISTA instrument. Geophysical Research Letters, 2003, 30, .	4.0	48
20	A decadal satellite record of gravity wave activity in the lower stratosphere to study polar stratospheric cloud formation. Atmospheric Chemistry and Physics, 2017, 17, 2901-2920.	4.9	48
21	Instrument concept and preliminary performance analysis of GLORIA. Advances in Space Research, 2006, 37, 2287-2291.	2.6	47
22	Measurements of trace gases by the cryogenic infrared spectrometers and telescopes for the atmosphere (CRISTA) experiment. Advances in Space Research, 1997, 19, 563-566.	2.6	46
23	CRISTA-2 observations of the South Polar Vortex in winter 1997: A new dataset for polar process studies. Geophysical Research Letters, 2001, 28, 3159-3162.	4.0	42
24	Stratospheric transport by planetary wave mixing as observed during CRISTA-2. Journal of Geophysical Research, 2002, 107, CRI 7-1-CRI 7-13.	3.3	39
25	A climatology of polar stratospheric cloud composition between 2002 and 2012 based on MIPAS/Envisat observations. Atmospheric Chemistry and Physics, 2018, 18, 5089-5113.	4.9	38
26	Indications of convectively generated gravity waves in crista temperatures. Advances in Space Research, 2001, 27, 1653-1658.	2.6	37
27	Fast cloud parameter retrievals of MIPAS/Envisat. Atmospheric Chemistry and Physics, 2012, 12, 7135-7164.	4.9	37
28	Satellite observations of cirrus clouds in the Northern Hemisphere lowermost stratosphere. Atmospheric Chemistry and Physics, 2015, 15, 927-950.	4.9	37
29	Observations of PAN and its confinement in the Asian summer monsoon anticyclone in high spatial resolution. Atmospheric Chemistry and Physics, 2016, 16, 8389-8403.	4.9	36
30	High resolution limb observations of clouds by the CRISTA-NF experiment during the SCOUT-O3 tropical aircraft campaign. Advances in Space Research, 2008, 42, 1765-1775.	2.6	32
31	Volcanic ash detection with infrared limb sounding: MIPAS observations and radiative transfer simulations. Atmospheric Measurement Techniques, 2014, 7, 1487-1507.	3.1	30
32	CRISTA-NF measurements of water vapor during the SCOUT-O3 Tropical Aircraft Campaign. Advances in Space Research, 2009, 43, 74-81.	2.6	28
33	An assessment of tropopause characteristics of the ERA5 and ERA-Interim meteorological reanalyses. Atmospheric Chemistry and Physics, 2022, 22, 4019-4046.	4.9	27
34	On the discrepancy of HCl processing in the core of the wintertime polar vortices. Atmospheric Chemistry and Physics, 2018, 18, 8647-8666.	4.9	26
35	Retrieval of CFC-11 and CFC-12 from Envisat MIPAS observations by means of rapid radiative transfer calculations. Advances in Space Research, 2005, 36, 915-921.	2.6	24
36	Chemical ozone loss and related processes in the Antarctic winter 2003 based on Improved Limb Atmospheric Spectrometer (ILAS)–II observations. Journal of Geophysical Research, 2006, 111, .	3.3	24

REINHOLD SPANG

#	Article	IF	CITATIONS
37	MIPAS detection of cloud and aerosol particle occurrence in the UTLS with comparison to HIRDLS and CALIOP. Atmospheric Measurement Techniques, 2012, 5, 2537-2553.	3.1	24
38	A stratospheric intrusion at the subtropical jet over the Mediterranean Sea: air-borne remote sensing observations and model results. Atmospheric Chemistry and Physics, 2012, 12, 8423-8438.	4.9	24
39	Infrared limb emission measurements of aerosol in the troposphere and stratosphere. Atmospheric Measurement Techniques, 2016, 9, 4399-4423.	3.1	24
40	Scattering in infrared radiative transfer: A comparison between the spectrally averaging model JURASSIC and the line-by-line model KOPRA. Journal of Quantitative Spectroscopy and Radiative Transfer, 2013, 127, 102-118.	2.3	23
41	CRISTA-NF measurements during the AMMA-SCOUT-O3 aircraft campaign. Atmospheric Measurement Techniques, 2010, 3, 1437-1455.	3.1	22
42	MIPAS observation of polar stratospheric clouds in the Arctic 2002/2003 and Antarctic 2003 winters. Advances in Space Research, 2005, 36, 868-878.	2.6	21
43	A multi-wavelength classification method for polar stratospheric cloud types using infrared limb spectra. Atmospheric Measurement Techniques, 2016, 9, 3619-3639.	3.1	21
44	How homogeneous and isotropic is stratospheric mixing? Comparison of CRISTA-1 observations with transport studies based on the Chemical Lagrangian Model of the Stratosphere (CLaMS). Quarterly Journal of the Royal Meteorological Society, 2005, 131, 565-579.	2.7	20
45	Stratospheric lifetime ratio of CFC-11 and CFC-12 from satellite and model climatologies. Atmospheric Chemistry and Physics, 2014, 14, 12479-12497.	4.9	20
46	Lagrangian simulation of ice particles and resulting dehydration in the polar winter stratosphere. Atmospheric Chemistry and Physics, 2019, 19, 543-563.	4.9	13
47	Testing our understanding of Arctic denitrification using MIPAS-E satellite measurements in winter 2002/2003. Atmospheric Chemistry and Physics, 2006, 6, 3149-3161.	4.9	12
48	Observations of filamentary structures near the vortex edge in the Arctic winter lower stratosphere. Atmospheric Chemistry and Physics, 2013, 13, 10859-10871.	4.9	12
49	Spectroscopic evidence of large aspherical <i>β</i> -NAT particles involved in denitrification in the December 2011 Arctic stratosphere. Atmospheric Chemistry and Physics, 2016, 16, 9505-9532.	4.9	12
50	Radiance calibration of CRISTA-NF. Advances in Space Research, 2009, 43, 1910-1917.	2.6	11
51	A detection method for cirrus clouds using CRISTA 1 and 2 measurements. Advances in Space Research, 2001, 27, 1629-1634.	2.6	10
52	CFC11 measurements by CRISTA. Advances in Space Research, 1997, 19, 575-578.	2.6	9
53	A correlation study of highâ€altitude and midaltitude clouds and galactic cosmic rays by MIPASâ€Envisat. Journal of Geophysical Research, 2010, 115, .	3.3	8
54	Polar stratospheric clouds initiated by mountain waves in a global chemistry–climate model: a missing piece in fully modelling polar stratospheric ozone depletion. Atmospheric Chemistry and Physics, 2020, 20, 12483-12497.	4.9	8

REINHOLD SPANG

#	Article	IF	CITATIONS
55	Empirical evidence for deep convection being a major source of stratospheric ice clouds over North America. Atmospheric Chemistry and Physics, 2021, 21, 10457-10475.	4.9	7
56	Meteorological conditions of the stratosphere for the CRISTA 2 campaign, August 1997. Journal of Geophysical Research, 2002, 107, CRI 12-1-CRI 12-10.	3.3	6
57	Aerosol and cloud top height information of Envisat MIPAS measurements. Atmospheric Measurement Techniques, 2020, 13, 1243-1271.	3.1	6
58	The MIPAS/Envisat climatology (2002–2012) of polar stratospheric cloud volume density profiles. Atmospheric Measurement Techniques, 2018, 11, 5901-5923.	3.1	5
59	Observation of cirrus clouds with GLORIA during the WISE campaign: detection methods and cirrus characterization. Atmospheric Measurement Techniques, 2021, 14, 3153-3168.	3.1	5
60	A global view on stratospheric ice clouds: assessment of processes related to their occurrence based on satellite observations. Atmospheric Chemistry and Physics, 2022, 22, 6677-6702.	4.9	5
61	Level 2 near-real-time analysis of MIPAS measurements on ENVISAT. , 2003, , .		4
62	The benefit of limb cloud imaging for infrared limb sounding of tropospheric trace gases. Atmospheric Measurement Techniques, 2009, 2, 287-298.	3.1	4
63	Retrieval of chlorofluorocarbon distributions from Envisat MIPAS measurements. , 2004, , .		3
64	Cirrus cloud shape detection by tomographic extinction retrievals from infrared limb emission sounder measurements. Atmospheric Measurement Techniques, 2020, 13, 7025-7045.	3.1	3
65	Three-dimensional model simulations of CRISTA trace gas measurements. Advances in Space Research, 2000, 26, 971-974.	2.6	2
66	Horizontal temperature variability in the stratosphere: global variations inferred from CRISTA data. Advances in Space Research, 2001, 27, 1641-1646.	2.6	2
67	A new method to detect and classify polar stratospheric nitric acid trihydrate clouds derived from radiative transfer simulations and its first application to airborne infrared limb emission observations. Atmospheric Measurement Techniques, 2021, 14, 1893-1915.	3.1	2
68	Exploration of machine learning methods for the classification of infrared limb spectra of polar stratospheric clouds. Atmospheric Measurement Techniques, 2020, 13, 3661-3682.	3.1	2
69	Comparison of the CIRA 1990 planetary wave model to rocket temperature measurements. Advances in Space Research, 1996, 18, 347-350.	2.6	0
70	Do Galactic Cosmic Rays Impact the Cirrus Cloud Cover?. Springer Atmospheric Sciences, 2013, , 79-87.	0.3	0